Skull shape differentiation of black and white olms (*Proteus anguinus anguinus* and *Proteus a. parkelj*): an exploratory analysis with micro-CT scanning

Ana Ivanović[1, 4], Gregor Aljančič[2], Jan W. Arntzen[3]

[1] *Faculty of Biology, Institute for Zoology, University of Belgrade, Studentski trg 16, 11000 Belgrade, Serbia*
[2] *Tular Cave Laboratory, Oldhamska c. 8a, 4000 Kranj, Slovenia*
[3] *Naturalis Biodiversity Center, P.O. Box 9517, 2300 RA Leiden, The Netherlands*
[4] *E-mail: ana@bio.bg.ac.rs*

Key words: cranial skeleton, geometric morphometrics, Proteidae, troglomorphism

Abstract

We performed an exploratory analysis of the morphology of the cranium in the white olm (*Proteus anguinus anguinus*) and the black olm (*P. a. parkelj*) with micro-CT scanning and geometric morphometrics. The mudpuppy (*Necturus maculosus*) was used as an outgroup. The black olm falls outside the white olm morphospace by a markedly wider skull, shorter vomers which are positioned further apart and by laterally positioned squamosals and quadrates relative to the palate (the shape of the buccal cavity). On account of its robust skull with more developed premaxillae a shorter otico-occipital region, the black olm is positioned closer to *Necturus* than are the studied specimens of the white olm. The elongated skull of the white olm, with an anteriorly positioned jaw articulation point, could be regarded as an adaptation for improved feeding success, possibly compensating for lack of vision. As yet, the alternative explanations on the evolution of troglomorphism in *Proteus* are an extensive convergence in white olms versus the reverse evolution towards less troglomorphic character states in the black olm. To further understand the evolutionary trajectories within *Proteus* we highlight the following hypotheses for future testing: i) morphological differentiation is smaller within than between genetically differentiated white olm lineages, and ii) ontogenetic shape changes are congruent with the shape changes between lineages. We anticipate that the morphological detail and analytical power that come with the techniques we here employed will assist us in this task.

Contents

Introduction

The olm, *Proteus anguinus* Laurenti, 1768, is a unique obligate troglobiontic vertebrate species that inhabits underground waters of the Dinaric karst in the Balkan region of Europe. Its range is restricted to a narrow strip along the Adriatic coast, from the Isonzo / Soča River near Trieste in north-eastern Italy, through southern Slovenia, along the Adriatic coast of Croatia, to the Trebišnjica River in eastern Bosnia and Herzegovina (Sket, 1997; Parzefall *et al*., 1999; Fig. 1A). The species is divided into two subspecies based on the extent of troglomorphism as: i) the relatively widespread *Proteus a. anguinus* and ii) the recently discovered *P. a. parkelj* Sket and Arntzen, 1994, that is only known from the springs of three adjoining streams near Črnomelj in the region of Bela Krajina, southeastern Slovenia (Aljančič *et al*., 1986; Sket, 1993; Ivanović, 2012). We will refer to the two forms as the 'white olm' and the 'black olm', respectively. The nominotypical subspecies is characterized by undeveloped eyes that are covered by skin and the absence of skin pigmentation whereas the black olm possesses small, but well-developed eyes and is densely pigmented. The forms also differ in broad morphology, most markedly in the shape of the head, dentation and in the number of the costal groves (Sket and Arntzen, 1994; Arntzen and Sket, 1997). *Proteus anguinus* possesses an extremely anguiform body, with a unique position in the morphospace of European salamander species. Other anguiform Palearctic salamanders such as *Chioglossa lusitanica* Bocage, 1864 and *Mertensiella caucasica* Waga, 1876 have a short trunk and a long tail whereas *P. anguinus* has a long trunk and a
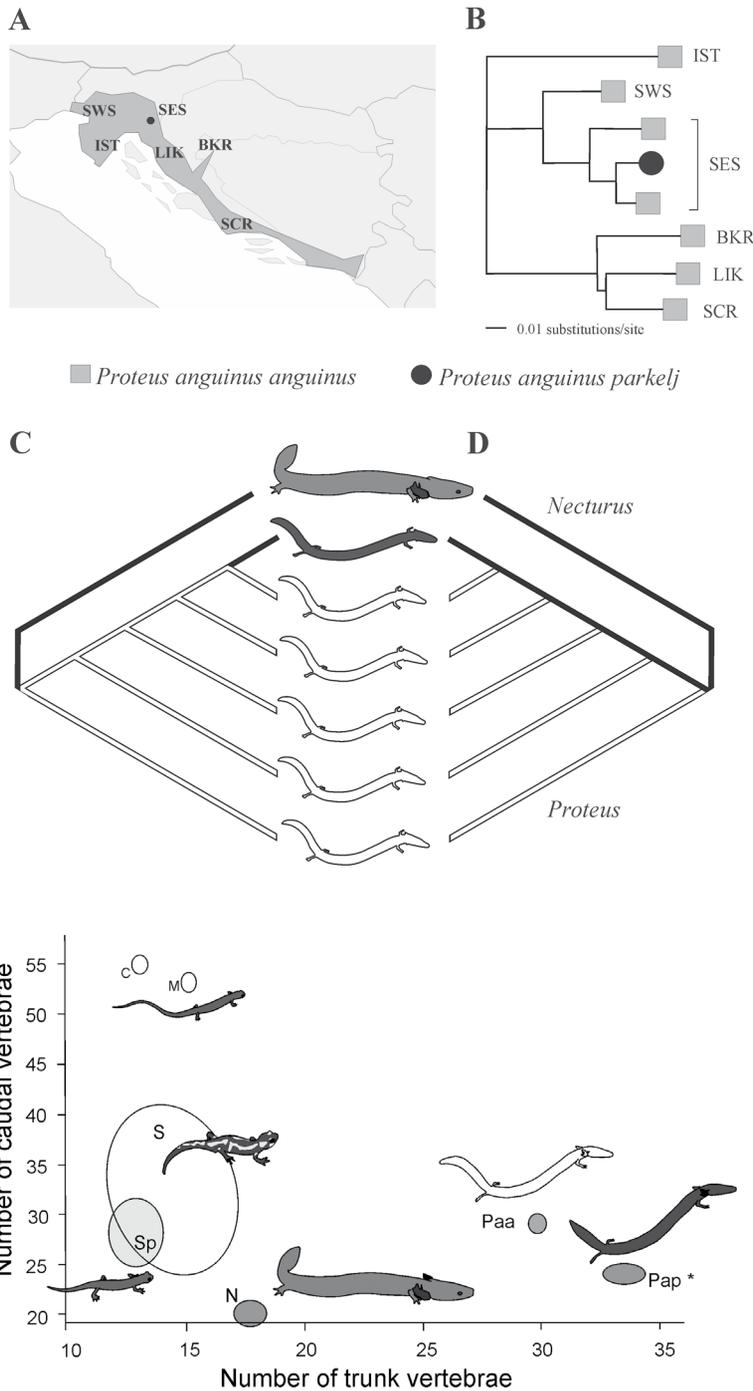
Fig. 1. Distribution of *Proteus anguinus* including the area of Dinaric karst in the Balkan region of Europe (A, after Parzefall *et al*., 1999; Sket, 1997), with (B) the nesting of genetic lineages (IST – Istria, SWS – Southwestern Slovenia, SES – Southeastern Slovenia, BKR – Bosanska Krajina, LIK – Lika, SCR – Southern Coastal Region), as revealed by nuclear loci (allozymes, Sket and Arntzen, 1994) and mitochondrial DNA sequences (Gorički and Trontelj, 2006; Trontelj *et al*., 2007). The phylogeny shown is after the latter papers. Alternative evolutionary scenarios that explain the troglomorphic (white) versus non-troglomorphic (black) character state distribution involve either the loss and subsequent gain (C, two evolutionary steps), or the multiple loss of the non-troglomorphic character conditions (D, five steps). We acknowledge that intermediate scenarios with three or more steps are also possible.

Fig. 2. Schematic representation of numbers of trunk vertebrae (horizontal axis) and caudal vertebrae (vertical axis) in Proteidae - *Necturus maculosus* (N), *Proteus anguinus anguinus* (Paa) and *Proteus anguinus parkelj* (Pap); Plethodontidae (*Speleomantes* species, Sp) and European representatives of the family Salamandridae (S); the exceptionally long tailed *Chioglossa lusitanica* (C) and *Mertensiella caucasica* (M) are shown separately. Data from Baur (1897), Lanza, Arntzen and Gentile (2010), Sket and Arntzen (1994). The ellipses encompass the variation in modal (horizontal) and mean values (vertical) observed for the group. * In the absence of observations, the number of caudal vertebrae was estimated through comparison with the interlimb-distance and tail length in *P. a. anguinus* in Arntzen and Sket (1997).

short tail (Fig. 2). As expressed by the number of trunk vertebrae, the black olm has an even longer body than the white olm.

Nuclear encoded genetic data (Sket and Arntzen, 1994) strongly suggest that the black olm is nested within a genetically diverged array of white olm populations. A wider phylogeographic study shows that white olm (*P. a. anguinus*) represents several deeply diverged lineages (six clades, based on mitochondrial DNA sequence data, Fig. 1B) and confirms that the black olm

lineage (*P. a. parkelj*) is deeply nested within white olm lineages (Gorički and Trontelj, 2006; Gorički *et al.*, 2012). Genetically the black olm is most similar to the white olm from the so-called SE Slovenia clade (*e.g.*, Otovski Breg, 2.5 km to the northeast of Jelševnik; Gorički and Trontelj, 2006).

The nested pattern of descent gives rise to two mutually exclusive evolutionary scenarios involving i) the origin of troglomorphism and the subsequent reverse evolution of the non-troglomorphic (or less-troglomorphic) condition in the black olm (Fig. 1C), or ii) the independent evolution of the troglomorphic condition in multiple lineages of the white olm (Fig. 1D). Arguments in support of the latter explanation are twofold. First, a marked geographic structuring and isolation by paleo-hydrographic units (Sket and Arntzen, 1994; Arntzen and Sket, 1997; but see also Grillitsch and Tiedemann, 1994), and the deep genetic separation of geographically separated lineages of the white olm are suggesting their independent evolutionary trajectories (Gorički *et al.*, 2012). Secondly and more general, it is well-documented that underground habitats promote evolutionary convergence (Wiens *et al.*, 2003; Jeffery, 2008; see also Pipan and Culver, 2012). Under this hypothesis, the extent of morphological uniformity of several white olm lineages would make *Proteus* a prime example of convergent evolution. It raises the question why and how the black olm lineage regained (Fig. 1C) or retained (Fig. 1D) ancestral, less troglomorphic character states.

The cranial skeleton carries important information related to jaw movement mechanics involved in feeding, competitive, reproductive and anti-predatory behaviour (Hanken and Hall, 1993) and refuge use (Herrell *et al.*, 2001, 2007). Even small differences in cranium size and shape may have important biomechanical and ecological implications (Herrell *et al.*, 2001, 2007; Verwaijen *et al.*, 2002; van der Meij and Bout, 2008). The skull of *Proteus* is narrow, elongate and dorsoventrally flattened (Trueb, 1993). The most detailed description of the *Proteus anguinus* skull yet is that of Dolivo-Dobrovolsky (1923, 1926), however, with limited data on variation in skull shape within *Proteus*. Indeed, the four specimens that Dolivo-Dobrovolsky (1926) used for his reconstruction were from the localities of Vir and Luče, Slovenia and represent the SE Slovenia clade.

The present paper aims to reduce a gap in our knowledge by the description of *Proteus* skulls from the black and white subspecies. To this end, information obtained with a micro-CT scanner was analyzed with the geometric morphometric approach. This combination of hard- and software is uniquely suited to detect even subtle differences in shape and has already been successfully used in a wide range of evolutionary, developmental, ecological and taxonomic studies (*e.g.* Zelditch *et al.*, 2012), on a variety of organisms including amphibians (Wilkinson *et al.*, 2011; Sherratt *et al.*, 2012). With this approach we captured the cranial morphology of black and white *Proteus* with unprecedented detail. Based on the descriptions, we propose several lines of research that would help to better understand morphological evolution in *Proteus*.

Material and methods

From material available at the collection of the Naturalis Biodiversity Center we studied six specimens of *P. a. anguinus* [ZMA.RenA.6381 a and b (total length, L = 205 mm, 260 mm) from Planinska Jama, ZMA.RenA.9045 a and b (L = 195 mm, 170 mm) from 'Postojna', ZMA.RenA.22200 (L = 195 mm) from 'Karst Krain', ZMA.RenA.21616 (L = 210 mm) from 'Triest' and one *Proteus anguinus parkelj* ZMA.RenA.9239 from Jelševnik, Slovenia (L = 230 mm, paratype). Four white olm specimens (ZMA.RenA.6381 a and b, ZMA.RenA.9045 a and b) represent the SW Slovenia clade [note that Postojna (or Postojnska) Jama and Planina (or Planinska) Jama belong to the same cave system] and one black olm specimen represents the SE Slovenia clade. For the two remaining white specimens (ZMA.RenA.22200 'Karst Krain' and ZMA.RenA.21616 'Triest'), the origins cannot be fully certified. 'Krain' refers to the Duchy of Carniola in today's central Slovenia while 'Karst' refers to the 'classical Karst' of southwestern Slovenia (Jones and White, 2012). We think that the material probably originates from the relatively easily accessible parts of the Postojna-Planina cave system. According to its label, the specimen from Triest 'died in the aquarium on May 6, 1930', 'don. [donated by] Suringar'. One more white *Proteus* (ZMA.RenA.22199, not studied by us) has a similar record ('Triest, leg. Suringar. Died at N. A. M. on October 26, 1932') where 'N. A. M.' stands for the Amsterdam Zoo Natura Artis Magistra and material from this Zoo normally went to the Amsterdam museum collection (ZMA, Zoological Museum Amsterdam, now merged with the collection of the Naturalis Biodiversity Center, Leiden). While this white olm specimen could be genuinely from the Trieste region (see Fig. 1) it is possible that the label is misleading, because olms from the Postojna-Planina cave were
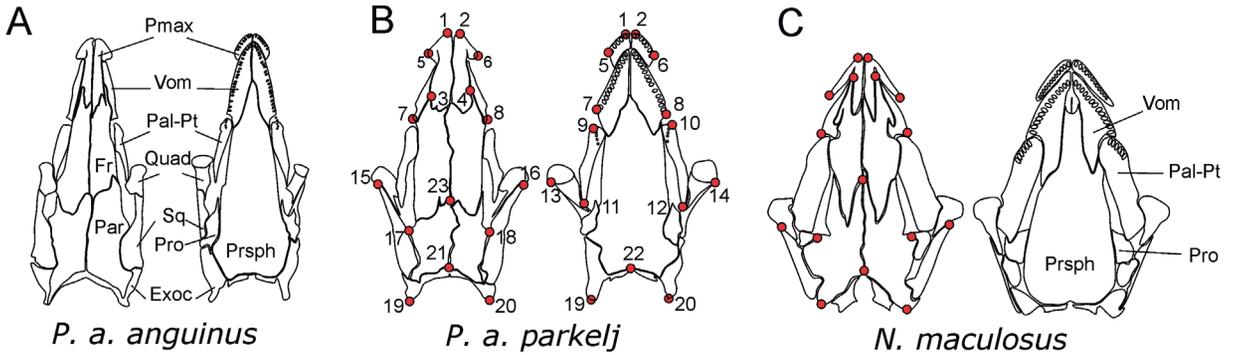
Fig. 3. Schematic representation of the dorsal (left) and ventral (right) views of *Proteus anguinus* and *Necturus maculosus* crania demonstrating differences in shape. A) *P. a. anguinus* (ZMA.RenA.6381a), B) *P. a. parkelj* (ZMA.RenA.9239) and C) *Necturus maculosus* skulls (TNHC 53001). Drawings are scaled to the same size. Pmax – premaxilla, Vom – vomer, Pal-Pt – palato-pterygoid, Quad – quadrate, Sq – squamosal, Pro – prootic, Exoc – exoccipital, Fr – frontal, Par – parietal and Prsph – parasphenoid. Solid dots represent 20 bilaterally symmetric and three medial landmarks used for 3D geometric morphometric analyses. A subset of 16 landmarks presented on the dorsal skull of *Necturus maculosus* was used for 2D geometric morphometric analyses.
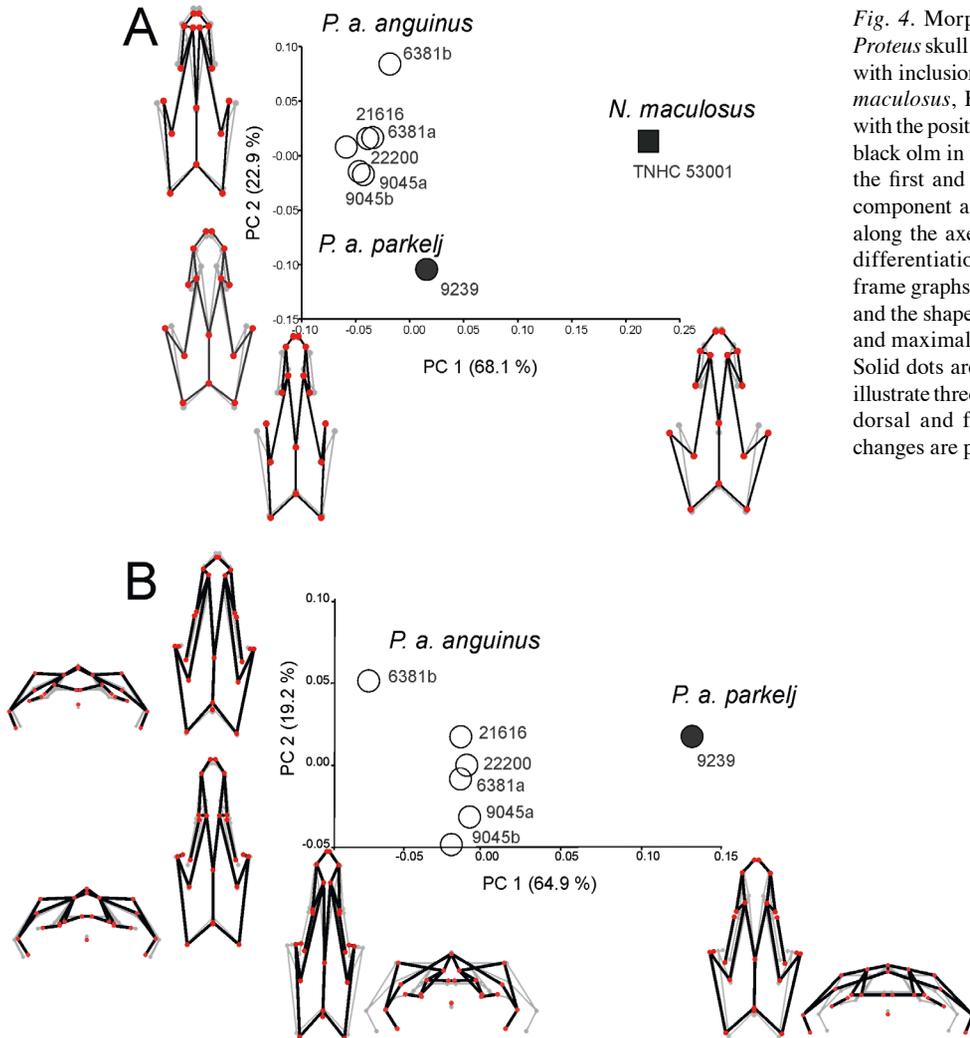

Fig. 4. Morphological variation in the *Proteus* skull as A) two dimensional shape, with inclusion of a specimen of *Necturus maculosus*, B) three dimensional shape with the position of six white olms and one black olm in the morphospace defined by the first and second axis from principal component analysis. Variation explained along the axes in %. The morphological differentiation is summarized by wire-frame graphs with the mean shape in grey and the shape of specimens with minimal and maximal scores on PC axes in black. Solid dots are landmarks as in Fig. 3. To illustrate three dimensional shape changes, dorsal and frontal projection of shape changes are presented.

frequently marketed in Trieste in the second half of 19th and first half of 20th century (Shaw, 1999).

The selected individuals were scanned with a Skyscan 1172 100 kV computed microtomograph (Skyscan, Aartselaar, Belgium) under the following settings: 74 kV, 0.8 rotation step, 515 ms exposure time, four frame averaging with no filter. At the two-dimensional (2D) reconstruction stage, the global threshold values were verified manually. The 3D surface models of the skulls were produced using the SkyScan CT-Analyser® 1.10 software, under a marching cube algorithm and a resolution of 26.1 μm. The morphometric analysis was based on a three-dimensional configuration of 23 landmarks (see Fig. 3 for landmark positions), obtained directly from the corresponding surface models with the software IDAV 3.0 (Institute of Data Analysis and Visualisation, University of California, Davis), and on a configuration of 16 landmarks scored on a two-dimensional projection of the dorsal side of the skull. To obtain a matrix of coordinates from which differences due to position, scale and orientation had been removed, we applied a Generalized Procrustes Analysis (GPA; see Zelditch *et al*., 2012 and references therein). By this approach, we eliminated the effect of size and we analysed the variation in cranium shape exclusively. As shape variables we used the symmetric component of shape variation (an average of the original and mirrored configuration for each specimen, Klingenberg *et al*., 2002). Although small samples sizes (N < 10) are frequently used in geometric morphometric studies, larger samples would provide a more accurate estimate of mean skull shape and shape variance (Cardini and Elton, 2007). Bearing this in mind, we performed an exploratory analysis with Principal Component Analysis (PCA), to visualise the position and variation in skull shape of the salamanders in the morphospace described by first two principal components. We calculated Mahalanobis distances between specimens and/or mean shapes with the software MorphoJ (Klingenberg, 2011). As an outgroup to our analyses we used imagery of the mudpuppy, *Necturus maculosus* Rafinesque, 1818, from the Texas Memorial Museum - Texas Natural History Collections (TNHC 53001). Data for *Necturus maculosus* are available at: http://digimorph.org/specimens/Necturus_maculosus/whole/ and were accessed on January 2, 2012.

Results

In comparison with the studied material of the white olm (*P. a. anguinus*), the black olm (*P. a. parkelj*) has a more robust skull, with a wider snout resulting from laterally extended and more developed premaxillae and shorter vomers which are positioned further apart. The skull of the black olm is considerably wider at the jaw articulation point and has a rhomboid shape, compared to the elongated and nearly triangular skull of the white olm (Fig. 3). The dental part of the praemaxilla and the wing-shaped part of the premaxilla that projects dorsally and overlaps with the frontal bone are more robust and more developed in the black than in the white olm. The dental part of praemaxilla has 8-10 premaxillary teeth in the white and 6-7 in the black olm. The premaxillary bones form an angle in the range of 65-81° in white olms and is 92° in the black olm. The vomerine teeth are organised in single series along each vomer. There are 22-30 vomerine teeth in the white and 16-17 in the black olm. The angle between the teeth rows ranges from 30-40° in the white and is 54° in the black olm. The paired palato-pterygoid bone bears much smaller teeth, and the number was difficult to determine exactly at the given resolution. In white olms there are up to 6 palato-pterygoid teeth and they could be absent on one side (ZMA.RenA.9045a, ZMA.RenA.21616). These teeth are aligned with the arch of the vomerine teeth. In the black olm the palato-pterygoid bone bears 5-6 teeth which have a different alignment compared to the white olm (oriented transversally to the vomerine teeth at approximately 35°).

The configuration of 16 landmarks that cover the dorsal skull shape reflects the general shape as well as the relationship between bones that form the snout and skull roof (premaxillar, frontal and parietal bones), squamosal and the otico-occipital regions. The first and second principal component axes together explain just over 90% of the total variation in dorsal skull shape in the 2D data (Fig. 4A). The outgroup *Necturus maculosus* separates along the first PCA-axis from both the white (*P. a. anguinus*) and black olm (*P. a. parkelj*), on account of its robust skull. The positions of the specimens in morphospace described by the first and the second axis reveal that white *Proteus* specimens have a narrower and a more elongated skull with a more anteriorly positioned jaw articulation point, compared to the black *Proteus* specimen. Among white olm specimen ZMA.RenA.6381b falls well outside the variation of the remaining *P. a. anguinus*. This individual has the narrowest snout and most anteriorely positioned lateral suture of premaxillar and frontal bones. The Mahalanobis distance (D_M) is $D_M = 12.59$ between *Necturus maculosus* and the mean for *P. a. anguinus*; $D_M = 9.28$ for *Necturus maculosus* and *P. a. parkelj* and $D_M = 5.41$ for *P. a. anguinus* and *P. a. parkelj*.
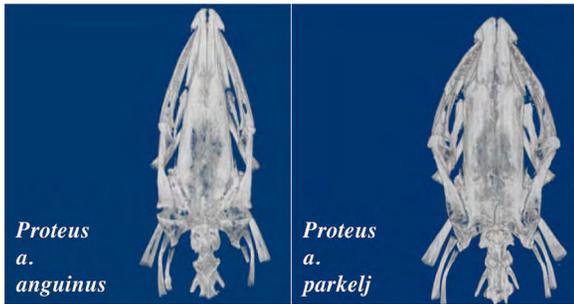
Fig. 5. Three dimensional view of *Proteus a. anguinus* (ZMA. RenA**.**21616) and *Proteus a. parkelj* (ZMA.RenA.9239) cranial skeleton. Click the link for video representation.

The 3D dataset shows a similar relationship between *P. a. parkelj* and *P. a. anguinus* as the 2D dataset while it also uncovers information on the skull geometry of the two forms. The observed variation within the studied material of the white olm is related to the change in the lateral suture of premaxillar and frontal bones and to the position of the palato-pterygoid relative to the vomers (Fig. 4B). The relative position of squamosals and quadrates clearly separate the white olms from the black one. White olms have anteriorely placed and almost vertically positioned squamosals compared to the black olm. These changes, along with changes in the shape of the snout and a general narrowing/widening of the entire skull, affect the shape of the buccal cavity (Fig. 4B and Fig. 5).

Discussion and conclusion

We documented a different skull morphology for the white olm (*Proteus a. anguinus)* and the black olm (*Proteus a. parkelj*) with unprecedented detail. The black olm falls outside the observed white olm range by a wider skull (in particular at the level of the jaw articulation) and shorter skull, a wider snout with more developed premaxillae and shorter vomers which are positioned further apart. The black olm is positioned closer to the *Necturus* than is the white olm, which is largely due to its more robust dorsal cranial skeleton. The differences between black and white olm in the position of the jaw articulation point and in the shape of the buccal cavity could be related to divergences in feeding performance. Both genera (*Proteus* and *Necturus*) have larval skull features (Duellman and Trueb, 1986; Deban and Wake, 2000; Rose, 2003), and they feed by suction (Trueb, 1993; Deban and Wake, 2000). In suction feeding salamanders, the long

and narrow snout generates a more powerful suction produced by the hyobranchial apparatus (Trueb, 1993). The narrower and elongated skull of *P. a. anguinus* with a more anteriorely positioned jaw articulation point, compared to the *P. a. parkelj* and *Necturus maculosus* may be interpreted as an adaptation towards feeding in the dark, when attacks are unguided by vision. As has been noted, for salamanders in the genus *Plethodon*, even small differences in skull shape can be indicative of change in feeding performance (Adams and Rohlf, 2000). Unfortunately, empirical data and comparative studies on form and function in aquatic amphibians are sparse (Deban and Wake, 2000) and the Proteidae are no exception.

The general characteristics of subterranean ecosystems contribute to the evolution of morphologically cryptic species (Wiens *et al.*, 2003; Trontelj *et al.*, 2009). This observation seems to apply to the white *Proteus* lineages that are morphologically similar, yet genetically distinct (Sket and Arntzen, 1994; Gorički and Trontelj, 2006). Convergent evolution of troglobiont populations is well documented in the Mexican tetra *Astyanax mexicanus* (De Filippi, 1853). Among numerous phenotypic traits, cave-dwelling populations of this species differ in morphology from surface-dwelling populations by reduction or loss of eyes and pigmentation, a smaller number of trunk vertebrae, less developed visual centres, brain size and shape (Yamamoto *et al.*, 2003; Jeffery, 2008). Both positive selection and indirect selection, based on antagonistic pleiotropy between regressive traits (eye loss) and constructive traits (other sensory system such as an increase in number and size of the taste buds and neuromasts), as well as an accumulation of neutral mutations have been recognized as mechanisms that operate on troglobiont populations in the Mexican tetra (Jeffery, 2008). The black *Proteus* is characterized by several undoubtedly ancestral character states (pigmentation and the presence of eyes). In the more troglomorphic white olm, pigment loss and several morphological changes have occurred (eye reduction and changes in the shape of the cranial skeleton - narrowing and elongation of the skull, a parallel position of the vomers and change of the position of jaw articulation point). Also, white *Proteus* have a lower number of trunk vertebrae compared to the black *Proteus* (three to four units difference; Arntzen and Sket, 1994), with a distinct position for both in the salamander morphospace (Fig. 2).

Such pattern of variation indicates the convergent evolution of several morphological traits. The length of time available for a white *Proteus* to achieve its troglomorphic phenotype has been estimated at 9-5 Ma (million years) from the level of nuclear genetic differen-

tiation (Sket and Arntzen, 1994) and at 16-5 Ma from mitochondrial DNA divergence (Trontelj *et al*., 2007; Goricki *et al*., 2012). The minimum time estimated from the last common ancestor of the black and white olm sister-lineages is 2.4-1.1 Ma or 0.6-0.5 Ma, depending on the mitochondrial DNA region studied (Goricki and Trontelj, 2006).

Among white olms, the discrete position of specimen ZMA.RenA.6381b, due to its narrow snout and most anteriorely positioned lateral suture of premaxillar and frontal bones, is perhaps best explained by allometric changes. With 260 mm total length it is the largest specimen we studied and presumably the only adult in our sample. Limited data from a captive population at the Tular Cave Laboratory show that *Proteus* in the size range of 170-230 mm are at the onset of sexual maturity (GA, unpublished data).

Our results show a high sensitivity of the applied techniques in revealing divergences and variation in *Proteus* skull shape. Further studies might focus on the prevalence of clinal geographical variation (Grillitsch and Tiedemann, 1994) versus a pattern of isolation by paleo-hydrographic units and intensive karstification (Sket and Arntzen, 1994; Sket, 1997; Trontelj *et al*., 2007). The prime question is if the lineages of white *Proteus* - in spite of evolutionary convergence - can be distinguished on the basis of skull shape. We anticipate that further studies on morphological variation and ontogenetic shape change from a larger dataset with more black olms and many more white olms of the genetically differentiated lineages, will provide insight into the patterns and mechanisms of morphological evolution (*i.e.*, differentiation versus stasis) of *Proteus* and the evolution of skull shape within Proteid salamanders in general. We conclude that CT-scanning is a promising tool to study morphological divergence of *Proteus* lineages. In particular we look forward to data that would test the hypothesis that white olm lineages are not just genetically, but also morphologically distinguishable. We anticipate that niche occupation will come into play as an explanatory variable to shed light on this enigmatic species and to why the black olm has not converged to troglobiont life as much as did the various white olm lineages.

Acknowledgements

References

Adams DC, Rohlf FJ. 2000. Ecological character displacement in *Plethodon*: biomechanical differences found from a geometric morphometric study. *Proceedings of the National Academy of Science of United States of America* 97: 4106-4111.

Aljancic M, Habic P, Mihevc A. 1986. Crni moceril iz Bele krajine [The Black olm from White Carniola]. *Nase jame* 28: 39-44.

Arntzen JW, Sket B. 1997. Morphometric analysis of black and white European cave salamanders, *Proteus anguinus*. *Journal of Zoology, London* 241: 699-707.

Baur G. 1897. Remarks on the question of intercalation of vertebrae. *Zoological Bulletin* 1: 41-55.

Cardini A, Elton S. 2007. Sample size and sampling error in geometric morphometric studies of size and shape. *Zoomorphology* 126: 121-34.

Deban SM, Wake DB. 2000. Aquatic Feeding in Salamanders. Pp. 65-94, in: Schwenk K, ed., *Feeding: form, function and evolution in tetrapod vertebrates*. San Diego: Academic Press.

Dolivo-Dobrovolsky V. 1923. Das Kopfskelett des Grottenolmes (*Proteus anguinus* Laur.). *Zoologischer Anzeiger* 57: 281-284.

Dolivo-Dobrovolsky V. 1926. Lobanja cloveske ribice (*Proteus anguinus* Laurenti). *Rad Jugoslavenske akademije znanosti i umjetnosti* 232: 190-209.

Duellman WE, Trueb L. 1986. *Biology of amphibians*. New York: McGraw Hill.

Goricki S, Trontelj P. 2006. Structure and evolution of the mitochondrial control region and flanking sequences in the European cave salamander *Proteus anguinus*. *Gene* 378: 31-41.

Goricki S, Niemiller ML, Fenolio DB. 2012. Salamanders. Pp. 665-676 in: White WB, Culver DC, eds, *Encyclopedia of caves*. 2nd ed. Oxford: Academic Press.

Grillitsch H, Tiedemann F. 1994. Die Grottenolm-Typen Leopold Fitzingers (Caudata: Proteidae: *Proteus)*. *Herpetozoa* 7: 139-148.

Hanken J, Hall BK. 1993. Mechanisms of skull diversity and evolution. Pp. 1-36 in: Hanken J, Hall BK, eds, *The skull: functional and evolutionary mechanism*. Chicago: The University of Chicago Press.

Herrell A, Van Damme R, Vanhooydonck B, De Vree F. 2001. The implications of bite performance to diet in two species of lacertid lizards. *Canadian Journal of Zoology* 79: 662-670.

Herrell A, McBrayer LD, Larson PM. 2007. Functional basis for sexual differences in bite force in the lizard *Anolis carolinensis*. *Biological Journal of Linnean Society* 91: 111-119.

Ivanovic M. 2012. Novo odkritje tretje lokacije habitata crnega mocerila v Beli krajini [New discovery of the third locality of the black olm in Bela Krajina]. *N-vestnik* 9: 1-2.

Jeffery WR. 2008. Emerging model systems in evo-devo: cavefish and microevolution of development. *Evolution & Development* 10: 265-272.

Jones WK, White WB. 2012. Karst. Pp. 430-438 in: White WB, Culver DC, eds, *Encyclopedia of caves*. 2nd ed. Oxford: Academic Press.

Klingenberg CP. 2011. MorphoJ: an integrated software package for geometric morphometrics. *Molecular Ecology Resources* 11: 353-357.

Klingenberg CP, Barluenga M, Meyer A. 2002. Shape analysis of symmetric structures: quantifying variation among individuals and asymmetry. *Evolution* 56: 1909-1920.

Lanza B, Arntzen JW, Gentile E. 2010. Vertebral numbers in the Caudata of the western Palaearctic (Amphibia). *Atti del Museo Civico di Storia Naturale di Trieste* 54: 3-114.

Meij MA van der, Bout RG. 2008. The relationship between shape of the skull and bite force in finches. *The Journal of Experimental Biology* 211: 1668-1680.

Parzefall J, Durand JP, Sket B. 1999. *Proteus anguinus* Laurenti, 1768 - Grottenolm. Pp. 57-76 in: Schwanzlurche I, Grossenbacher K, Thismeier B, eds, *Handbuch der Reptilien und Amphibien Europas*. Wiesbaden: Aula Verlag.

Pipan T, Culver DC. 2012. Convergence and divergence in the subterranean realm: a reassessment. *Biological Journal of the Linnean Society* 107: 1-14.

Rose C. 2003. The developmental morphology of salamander skulls. Pp. 1684-1781 in: Heatwole H, Davies M, eds, *Amphibian Biology: Osteology*. Chipping Norton: Surrey Beatty and Sons, Pty. Ltd.

Shaw T. 1999. *Proteus* for sale and for science in the 19th century. *Acta Carsologica* 28: 229-304.

Sherratt E, Wilkinson M, Gower DJ, Klingenberg CP. 2012. Evolution of cranial modularity in caecilians. *Integrative and Comparative Biology* 52 (Supplement 1): E159.

Sket B. 1993. Nova rasa človeške ribice (Kako se "naredi" novo podvrsto ali članek o članku). [A new subspecies of olm (How to "make" a new subspecies, or an article about an article.] *Proteus* 56: 3-11.

Sket B. 1997. Distribution of *Proteus* (Amphibia: Urodela: Proteidae) and its possible explanation. *Journal of Biogeography* 24: 263-280.

Sket B, Arntzen JW. 1994. A black, non-troglomorphic amphibian from the karst of Slovenia: *Proteus anguinus parkelj* n. ssp. (Urodela: Proteidae). *Bijdragen tot de Dierkunde* 64: 33-53.

Trontelj P, Gorički Š, Polak S, Verovnik R, Zakšek V, Sket B. 2007. Age estimates for some subterranean taxa and lineages in the Dinaric Karst. *Acta Carsologica* 36: 183-189.

Trontelj P, Douady CJ, Fišer C, Giber J, Gorički Š, Lefébure T, Sket B, Zakšek V. 2009. A molecular test for cryptic diversity in ground water: how large are the ranges of macrostygobionts? *Freshwater Biology* 54: 727-744.

Trueb L. 1993. Patterns of cranial diversity among the Lissamphibia. Pp. 255-343 in: Hanken J, Hall BK, eds, *The skull: patterns of structural and systematic diversity*. Chicago: The University of Chicago Press.

Verwaijen D, van Damme R., Herrel A. 2002. Relationships between head size, bite force, prey handling efficiency and diet in two sympatric lacertid lizards. *Functional Ecology* 16: 842-850.

Wiens JJ, Chippindale PT, Hillis DM. 2003. When are phylogenetic analyses misled by convergence? A case study in Texas cave salamanders. *Systematic Biology* 52: 501-514.

Wilkinson M, San Mauro D, Sherratt E, Gower DJ. 2011. A nine-family classification of caecilians (Amphibia: Gymnophiona). *Zootaxa* 2874: 41-64.

Yamamoto Y, Espinasa L, Stock DW, Jeffery WR. 2003. Development and evolution of craniofacial patterning is mediated by eye-dependent and -independent processes in the cavefish *Astyanax*. *Evolution & Development* 5: 435-446.

Zelditch ML, Swiderski DL, Sheets DH. 2012. *Geometric Morphometrics for Biologists: A Primer*. 2nd ed. San Diego: Elsevier Academic Press.